The Price of Anarchy in Active Signal Landscape Map Building

Zaher M. Kassas and Todd E. Humphreys
Radionavigation Laboratory, Wireless Networking and Communications Group
The University of Texas at Austin
Austin, Texas, USA
zkassas@ieee.org, todd.humphreys@mail.utexas.edu

***Abstract*—Multiple receivers with *a priori* knowledge about their own initial states are assumed to be dropped in an unknown environment comprising multiple signals of opportunity (SOPs) transmitters. The receivers draw pseudorange observations from the SOPs. The receivers' objective is to build a high-fidelity signal landscape map of the environment, which would enable the receivers to navigate accurately with the aid of the SOPs. The receivers could command their own maneuvers and such commands are computed so to maximize the information gathered about the SOPs in a greedy fashion. Several information fusion and decision making architectures are possible. This paper studies the price of anarchy in building signal landscape maps to assess the degradation in the map quality should the receivers produce their own maps and make their own maneuver decisions versus a completely centralized approach. In addition, a hierarchical architecture is proposed in which the receivers build their own maps and make their own decisions, but share relevant information. Such architecture is shown to produce maps of comparable quality to the completely centralized approach.**

***Index Terms*—navigation, signals of opportunity, adaptive sensing, information fusion**

I. Introduction

To overcome the limitations of global navigation satellite systems (GNSS)-based navigation, a new paradigm, termed opportunistic navigation (OpNav), has been proposed [1]. OpNav aims to extract positioning and timing information from ambient radio frequency (RF) signals of opportunity (SOPs). OpNav treats all RF signals as potential SOPs, from GNSS signals to communications signals never intended as navigation sources. In collaborative OpNav (COpNav), multiple OpNav receivers share information to construct and continuously refine a global signal landscape [2].

The observability and estimability of COpNav environments comprising multiple receivers making pseudorange observations on multiple SOPs were analyzed in [3]–[5]. While observability is a Boolean property, i.e. it asserts whether a system is observable or not, it does not specify which trajectory is best for information gathering, and consequently estimability. To address this, receiver-controlled maneuvers were allowed, and an optimal closed-loop information-based greedy (i.e., single-step look-ahead) strategy was proposed for receiver motion planning [6]. Three information-theoretic measures were compared: D-optimality, A-optimality, and E-optimality. It was shown that all three strategies outperformed a receiver moving randomly or in a pre-defined trajectory. Among these measures, D-optimality outclassed A-optimality and E-optimality. In [7], the greedy strategy was extended to a multi-step look-ahead strategy. In [8], it was shown that with proper reformulation, the greedy innovation-based motion planning strategy can be cast into a tractable convex program, the solution of which is computationally efficient.

The work in [6]–[8] considered the case of a single receiver and the problem of simultaneous receiver localization and signal landscape mapping with one "anchor" SOP whose initial states are known *a priori*. This is conceptually analogous to robot simultaneous localization and mapping (SLAM). In contrast, this paper focuses on signal landscape mapping with multiple receivers. The following problem is considered. Multiple receivers with *a priori* knowledge about their own initial states (e.g., from GNSS observables) are dropped in a completely unknown environment comprising multiple terrestrial SOPs. The receivers draw pseudorange observations from the SOPs. The receivers' objective is to build a high-fidelity signal landscape map of the environment, enabling SOP-based navigation and removing the dependency on GNSS signals.

Several information fusion and decision making architectures are possible: (i) decentralized: each receiver builds its own map and makes its own maneuver decisions, (ii) centralized: the receivers send their observations to a fusion center that builds the map and makes maneuver decisions for all receivers, and (iii) hierarchical: each receiver builds its own *local* map and makes its own decisions, but shares relevant information with a fusion center that maintains a *global* map. Two variants of the hierarchical architecture are considered: with and without feedback from the fusion center to each receiver. This paper compares the fidelity of the maps produced by the four architectures and assesses performance via the game-theoretic notion known as the price of anarchy (PoA), which quantifies the degradation in the solution quality in a decentralized approach from a centralized one [9].

This paper is organized as follows. Section II describes the dynamics and observation model. Section III summarizes the extended information filter (EIF), which is utilized for optimal fusion. Section IV states the optimal greedy control (OGC) problem that commands the receivers maneuvers. Section V presents the various architectures. Section VI presents simulation results comparing the maps produced through the various architectures. Conclusions are discussed in Section VII.

II. Model Description

A. Dynamics Model

Consider a planar environment composed of N receivers that control their own maneuvers and M stationary SOPs. The ith receiver dynamics evolve according to

$$\boldsymbol{x}_{r_i}(k+1) = \mathbf{F}_r\,\boldsymbol{x}_{r_i}(k) + \mathbf{G}_r\,\boldsymbol{u}_{r_i}(k) + \boldsymbol{w}_{r_i}(k),\ i = 1,\ldots,N$$

$$\mathbf{F}_r = \begin{bmatrix} \mathbf{I}_{2\times 2} & \mathbf{0}_{2\times 2} \\ \mathbf{0}_{2\times 2} & \mathbf{F}_{\rm clk} \end{bmatrix},\ \mathbf{G}_r = \begin{bmatrix} T\,\mathbf{I}_{2\times 2} \\ \mathbf{0}_{2\times 2} \end{bmatrix},\ \mathbf{F}_{\rm clk} = \begin{bmatrix} 1 & T \\ 0 & 1 \end{bmatrix}$$

where T is the sampling period, $\boldsymbol{x}_{r_i}^{\mathsf{T}} \triangleq \left[\boldsymbol{r}_{r_i}^{\mathsf{T}},\, \boldsymbol{x}_{{\rm clk},r_i}^{\mathsf{T}}\right]$ is the ith receiver state vector, which is composed of the planar position states $\boldsymbol{r}_{r_i}^{\mathsf{T}} \triangleq [x_{r_i},\, y_{r_i}]$ and the clock bias and drift states $\boldsymbol{x}_{{\rm clk},r_i}^{\mathsf{T}} \triangleq \left[\delta t_{r_i},\, \dot{\delta t}_{r_i}\right]$, $\boldsymbol{u}_{r_i}^{\mathsf{T}} \triangleq [u_{x,r_i},\, u_{y,r_i}]$ is the control input vector in the form of velocity commands, and $\boldsymbol{w}_{r_i}$ is the process noise vector, which is modeled as a zero-mean white noise sequence with covariance $\mathbf{Q}_{r_i}$, with $\mathbf{Q}_{r_i} = {\rm diag}\,[\mathbf{Q}_{p,r_i}, \mathbf{Q}_{{\rm clk},r_i}]$, $\mathbf{Q}_{p,r_i} = T\sigma_{p,r_i}^2\,\mathbf{I}_{2\times 2}$, where

$$\mathbf{Q}_{{\rm clk},r_i} = \begin{bmatrix} S_{\tilde{w}_{\delta t_{r_i}}} T + S_{\tilde{w}_{\dot{\delta} t_{r_i}}} \frac{T^3}{3} & S_{\tilde{w}_{\dot{\delta} t_{r_i}}} \frac{T^2}{2} \\ S_{\tilde{w}_{\dot{\delta} t_{r_i}}} \frac{T^2}{2} & S_{\tilde{w}_{\dot{\delta} t_{r_i}}} T \end{bmatrix},$$

where the clock bias and drift process noise power spectra $S_{\tilde{w}_{\delta t}}$ and $S_{\tilde{w}_{\dot{\delta} t}}$, respectively, can be related to the power-law coefficients, $\{h_\alpha\}_{\alpha=-2}^{2}$, which have been shown through laboratory experiments to characterize the power spectral density of the fractional frequency deviation of an oscillator from nominal frequency. It is common to approximate such relationships by considering only the frequency random walk coefficient h_{-2} and the white frequency coefficient h_0, which lead to $S_{\tilde{w}_{\dot{\delta} t}} \approx \frac{h_0}{2}$ and $S_{\tilde{w}_{\dot{\delta} t}} \approx 2\pi^2 h_{-2}$ [10].

The jth SOP dynamics evolve according to

$$\boldsymbol{x}_{s_j}(k+1) = \mathbf{F}_s\,\boldsymbol{x}_{s_j}(k) + \boldsymbol{w}_{s_j}(k), \quad j = 1,\ldots,M,$$

where $\mathbf{F}_s = {\rm diag}\,[\mathbf{I}_{2\times 2}, \mathbf{F}_{\rm clk}]$, $\boldsymbol{x}_{s_j}^{\mathsf{T}} \triangleq \left[\boldsymbol{r}_{s_j}^{\mathsf{T}},\, \boldsymbol{x}_{{\rm clk},s_j}^{\mathsf{T}}\right]$ is the jth SOP state vector, which is composed of the SOP's planar position states $\boldsymbol{r}_{s_j}^{\mathsf{T}} \triangleq \left[x_{s_j},\, y_{s_j}\right]$ and the SOP's clock bias and drift states $\boldsymbol{x}_{{\rm clk},s_j}^{\mathsf{T}} \triangleq \left[\delta t_{s_j},\, \dot{\delta t}_{s_j}\right]$, and $\boldsymbol{w}_{s_j}$ is the process noise vector, which is modeled as a zero-mean white noise sequence with covariance $\mathbf{Q}_{s_j}$, with $\mathbf{Q}_{s_j} = {\rm diag}\left[\mathbf{0}_{2\times 2}, \mathbf{Q}_{{\rm clk},s_j}\right]$, where $\mathbf{Q}_{{\rm clk},s_j}$ is identical to to $\mathbf{Q}_{{\rm clk},r_i}$, except that the spectra $S_{\tilde{w}_{\delta t_{r_i}}}$ and $S_{\tilde{w}_{\dot{\delta} t_{r_i}}}$ are now replaced with SOP-specific spectra, $S_{\tilde{w}_{\delta t_{s_j}}}$ and $S_{\tilde{w}_{\dot{\delta} t_{s_j}}}$, respectively.

B. Observation Model

The pseudorange observation made by the ith receiver on the jth SOP can be approximated by invoking mild approximations discussed in [3], [5], to yield the model

$$z_{r_i,s_j}(k) = h\left[\boldsymbol{x}_{r_i}(k), \boldsymbol{x}_{s_j}(k)\right] + v_{r_i,s_j}(k)$$

$$h\left[\boldsymbol{x}_{r_i}(k), \boldsymbol{x}_{s_j}(k)\right] \triangleq \|\boldsymbol{r}_{r_i}(k) - \boldsymbol{r}_{s_j}(k)\|_2 + c\cdot\left[\delta t_{r_i}(k) - \delta t_{s_j}(k)\right]$$

where c is the speed of light and v_{r_i,s_j} is the error in the pseudorange measurement due to modeling and measurement errors and is modeled as a zero-mean white Gaussian sequence with variance σ_{r_i,s_j}^2.

III. Extended Information Filter

For optimal fusion, the estimation scheme adopted to fuse estimates and associated estimation error covariances from multiple receivers making observations on the same SOPs cannot be formulated in the standard Kalman filter formulation, since this leads to suboptimal fusion [11]. However, by expressing the estimation problem in the information space instead of the state space, optimal fusion can be derived leading to the EIF [12], [13], a special case of which is summarized next.

Consider the linear dynamics and nonlinear observations

$$\begin{aligned} \boldsymbol{x}(k+1) &= \mathbf{F}\,\boldsymbol{x}(k) + \mathbf{G}\,\boldsymbol{u}(k) + \boldsymbol{w}(k) \\ \boldsymbol{z}(k) &= \boldsymbol{h}\left[\boldsymbol{x}(k)\right] + \boldsymbol{v}(k) \end{aligned}$$

where $\boldsymbol{x} \in \mathbb{R}^n$, $\boldsymbol{u} \in \mathbb{R}^r$, $\boldsymbol{w} \in \mathbb{R}^n$, $\boldsymbol{z} \in \mathbb{R}^m$, $\boldsymbol{v} \in \mathbb{R}^m$ are the system state, input, process noise, observation, and observation noise vectors, respectively. Assume $\boldsymbol{w}$ and $\boldsymbol{v}$ to be zero-mean, mutually-uncorrelated, white noise sequences with covariance matrices $\mathbf{Q}$ and $\mathbf{R}$, respectively.

Assume the initial knowledge about the system state to be captured in the state estimate $\hat{\boldsymbol{x}}(0|0)$ and associated estimation error covariance $\mathbf{P}(0|0)$. The EIF maintains the information state vector and information matrix, defined as $\hat{\boldsymbol{y}}(i|j) \triangleq \mathbf{Y}(i|j)\hat{\boldsymbol{x}}(i|j)$ and $\mathbf{Y}(i|j) \triangleq \mathbf{P}^{-1}(i|j)$, respectively, where $\hat{\boldsymbol{x}}(i|j)$ and $\mathbf{P}(i|j)$ are the state vector estimate and associated estimation error covariance at time i given all the observations up to and including time j. The EIF recursive prediction and correction equations are given by

$$\begin{aligned} \textbf{Prediction}\colon\ \hat{\boldsymbol{y}}(k+1|k) &= \mathbf{Y}(k+1|k)\left[\mathbf{F}\,\hat{\boldsymbol{x}}(k|k) + \mathbf{G}\,\boldsymbol{u}(k)\right] \\ \mathbf{Y}(k+1|k) &= \left[\mathbf{F}\,\mathbf{Y}^{-1}(k|k)\,\mathbf{F}^{\mathsf{T}} + \mathbf{Q}\right]^{-1} \\ \textbf{Correction}\colon\ \hat{\boldsymbol{y}}(k+1|k+1) &= \hat{\boldsymbol{y}}(k+1|k) + \boldsymbol{i}(k+1) \\ \mathbf{Y}(k+1|k+1) &= \mathbf{Y}(k+1|k) + \mathbf{I}(k+1), \end{aligned}$$

where $\boldsymbol{i}(k+1)$ and $\mathbf{I}(k+1)$ denote the information state contribution and its corresponding information matrix, respectively, associated with observation $\boldsymbol{z}(k+1)$, and are given by

$$\begin{aligned} \boldsymbol{i}(k+1) &= \mathbf{H}^{\mathsf{T}}(k+1)\mathbf{R}^{-1}\left[\boldsymbol{\nu}(k+1) + \mathbf{H}(k+1)\hat{\boldsymbol{x}}(k+1|k)\right] \\ \mathbf{I}(k+1) &= \mathbf{H}^{\mathsf{T}}(k+1)\mathbf{R}^{-1}\mathbf{H}(k+1) \\ \boldsymbol{\nu}(k+1) &= \boldsymbol{z}(k+1) - \boldsymbol{h}\left[\hat{\boldsymbol{x}}(k+1|k)\right], \end{aligned}$$

where $\mathbf{H}(k+1)$ is the Jacobian matrix evaluated at $\hat{\boldsymbol{x}}(k+1|k)$.

IV. Optimal Greedy Control

The OGC defines the optimal greedy maneuver $\boldsymbol{u}_{r_i}^{\star}(k)$ that receiver i must take so to minimize the constrained D-optimality criterion, which is equivalent to minimizing the volume of the uncertainty ellipsoid, given by

$$\begin{aligned} \underset{\boldsymbol{u}_{r_i}(k)}{\text{minimize}} \quad & \mathcal{J}\left[\boldsymbol{u}_{r_i}(k)\right] = \log\det[\mathbf{P}_i(k+1|k+1)] \\ \text{subject to} \quad & \|\boldsymbol{u}_{r_i}(k)\|_2 \le u_{r_i,\max} \\ & \|\boldsymbol{u}_{r_i}(k) - \boldsymbol{u}_{r_i}^{\star}(k-1)\|_2 \le T\,a_{r_i,\max}, \end{aligned} \tag{1}$$

where $u_{r_i,\max}$ and $a_{r_i,\max}$ are the maximum speed and acceleration, respectively, with which the receiver can move.

Note that the optimization vector is $\boldsymbol{u}_{r_i}(k)$, whereas $\boldsymbol{u}^{\star}_{r_i}(k-1)$ is a known constant vector representing the velocity commands that resulted from solving the optimization problem in the previous time-step $k-1$ and has already been applied.

V. Active Signal Landscape Map Building and Information Fusion Architectures

This section presents the various active signal landscape map building architectures. All architectures contain the following common blocks: (i) RF front-end (FE) processing and tracking loops (TL), (ii) extended information filter (EIF), (iii) optimal greedy control (OGC) solver, and (iv) receiver actuator to command the receiver maneuvers. The architectures are essentially classified according to where active decisions about the maneuvers are made, what information is communicated, and where the information is processed.

A. Decentralized

In this architecture (depicted in Fig. 1), each receiver acts individually: it fuses the observations made on the various SOPs to produce its own signal landscape map and makes its own decisions. The observations made by the ith receiver on all the SOPs in the environment are augmented into the vector $\boldsymbol{z}_i \triangleq [z_{r_i,s_1}, \cdots, z_{r_i,s_M}]^{\mathsf{T}}$, which is subsequently processed by the EIF to yield the *local* signal landscape state estimate $\hat{\boldsymbol{x}}_i(k|k)$ and associated estimation error covariance $\mathbf{P}_i(k|k)$. Based on these local estimates, each receiver solves for its own optimal greedy maneuver $\boldsymbol{u}^{\star}_{r_i}(k)$ defined in (1).

This architecture has the advantages of simplicity and self-containment, but suffers from the drawback that receivers do not exploit information gathered by other concurrent receivers.

B. Centralized

In this architecture (depicted in Fig. 2), the signal landscape map and decision making are made at a central fusion and decision center (CF & DC). The receivers send their observation vectors $\{\boldsymbol{z}_i\}_{i=1}^{N}$ to the CF & DC, which fuses such observations through an EIF to produce a *global* signal landscape map with estimate $\hat{\boldsymbol{x}}(k|k)$ and associated estimation error covariance $\mathbf{P}(k|k)$. The CF & DC OGC problem is identical to (1), except that it solves for the *global* optimal greedy maneuver for all receivers $\boldsymbol{u}^{\star}(k) \triangleq \left[[\boldsymbol{u}^{\star}_{r_1}(k)]^{\mathsf{T}}, \cdots, [\boldsymbol{u}^{\star}_{r_N}(k)]^{\mathsf{T}}\right]^{\mathsf{T}}$. The optimal maneuvers are communicated to each receiver.

This architecture is optimal; however, it requires two-way communication between the receivers and the CF & DC. Another drawback is that the CF & DC needs to solve a potentially large-scale OGC problem.

C. Hierarchical without Feedback

In this architecture (depicted in Fig. 3), the receivers produce their own signal landscape maps and make their own decisions. Additionally, they send their information vectors $\{\boldsymbol{i}_{r_i}\}_{i=1}^{N}$ and information matrices $\{\mathbf{I}_{r_i}\}_{i=1}^{N}$ to a central fusion center (CFC). The CFC is composed of an EIF, which maintains a *global* signal landscape map. The CFC EIF's prediction stage computations are made according to the EIF prediction equations given in Section III, while the correction stage computations are made according to

$$\hat{\boldsymbol{y}}(k+1|k+1) \;=\; \hat{\boldsymbol{y}}(k+1|k) + \sum_{i=1}^{N} \boldsymbol{i}_{r_i}(k+1)$$

$$\mathbf{Y}(k+1|k+1) \;=\; \mathbf{Y}(k+1|k) + \sum_{i=1}^{N} \mathbf{I}_{r_i}(k+1).$$

This architecture has the following advantages: (i) receivers possess their own local maps and (ii) a more accurate global map is available at the CFC. However, it suffers from the drawback that receivers have no access to the global map.

D. Hierarchical with Feedback

This architecture (depicted in Fig. 3), is identical to the one described in subsection V-C, except that once the CFC fuses the information from the various receivers to produce the *global* signal landscape map, such map is fed-back to each receiver to replace each receiver's local corrected map.

This architecture eliminates the drawback of the hierarchical without feedback architecture at the expense of requiring communication from the CFC to the receivers.

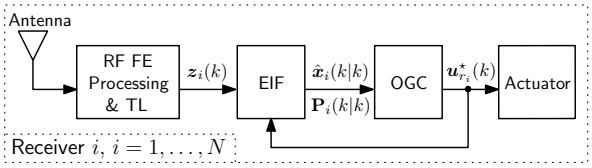

Fig. 1. Decentralized active signal landscape mapping and fusion architecture

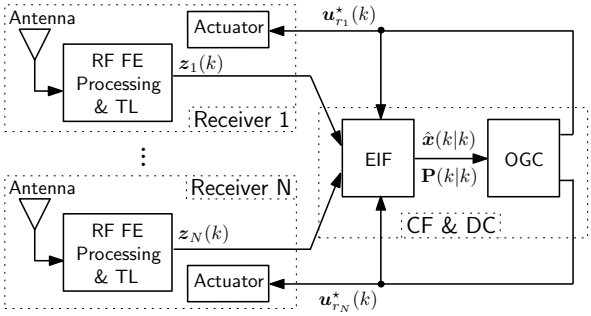

Fig. 2. Centralized active signal landscape mapping and fusion architecture

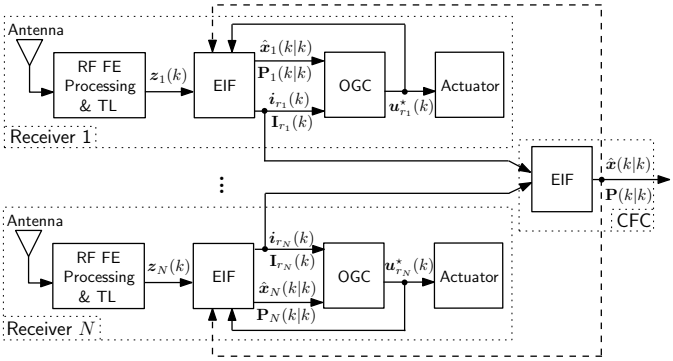

Fig. 3. Hierarchical active signal landscape mapping and fusion architecture with feedback and without feedback (no dashed line)

VI. Simulation Results

This section compares the architectures discussed in Section V numerically in an environment comprising two receivers whose initial states were chosen randomly and four SOPs. For purposes of numerical stability, the clock bias and drift states were defined as $c\delta t$ and $c\dot{\delta t}$, respectively. The receivers' and SOPs' clocks were assumed to be temperature-compensated and oven-controlled crystal oscillators (TCXOs and OCXOs), respectively. The simulation settings are given in Table I, where $i = 1, 2$ and $j = 1, \ldots, 4$.

TABLE I
Simulation Settings

Param.	Values	Param.	Values
$\boldsymbol{x}_{s_1}^{\mathsf{T}}(0)$	$[0, 150, 10, 0.1]$	$\mathbf{P}_{r_i}$	$10^4 \cdot \mathrm{diag}\,[1, 1, 1, 0.01]$
$\boldsymbol{x}_{s_2}^{\mathsf{T}}(0)$	$[100, -150, 20, 0.2]$	$\hat{\boldsymbol{x}}_{s_j}(0\vert 0)$	$\sim \mathcal{N}[\boldsymbol{x}_{s_j}(0), \mathbf{P}_{s_j}(0\vert 0)]$
$\boldsymbol{x}_{s_3}^{\mathsf{T}}(0)$	$[200, 200, 30, 0.3]$	$\mathbf{P}_{s_j}(0\vert 0)$	$10^4 \cdot \mathrm{diag}\,[1, 1, 1, 0.01]$
$\boldsymbol{x}_{s_4}^{\mathsf{T}}(0)$	$[-150, 50, 40, 0.4]$	h_{0,s_j}, h_{-2,s_j}	8×10^{-20}, 4×10^{-23}
$\boldsymbol{x}_{r_i}(0)$	$\sim \mathcal{N}[\bar{\boldsymbol{x}}_{r_i}, \mathbf{P}_{r_i}]$	h_{0,r_i}, h_{-2,r_i}	2×10^{-19}, 2×2^{-20}
$\bar{\boldsymbol{x}}_{r_1}^{\mathsf{T}}$	$[60, 15, 100, 10]$	$\sigma^2_{p,r_i}, \sigma^2_{r_i,s_j}$	$0.1\,(\mathrm{m/s^2})^2$, $500\,(\mathrm{m})^2$
$\bar{\boldsymbol{x}}_{r_2}^{\mathsf{T}}$	$[-55, 50, 100, 10]$	$T, u_{\max}, a_{\max}$	$0.1\,\mathrm{s}$, $10\,\mathrm{m/s}$, $5\,\mathrm{m/s^2}$

Fig. 4 compares the quality of the maps produced by the four architectures for a single run, as measured by the optimal value of the objective function, denoted $\mathcal{J}^\star$. Here, the same initial conditions and the same process and observation noise realizations were used. Fig. 5 shows the receivers trajectories due to the four architectures. Note that the trajectory for the hierarchical without feedback was identical to the decentralized, since receivers had no access to the global map.

The PoA is defined as the ratio of the objective function value worst case scenario and that of the optimal outcome. A PoA close to one means that the candidate solution is comparable to an optimal centralized one. The PoA was calculated as the ensemble average at the end of the simulation time for 25 Monte Carlo simulation runs, where the receivers' initial states, SOPs initial estimates, and noise realizations were randomized, and is tabulated in Table II. Note that, somewhat surprisingly, the hierarchial approach with feedback is comparable to a completely centralized approach.

TABLE II
Price of Anarchy

Architecture	Average	Standard Deviation
Decentralized	1.92	0.15
Hierarchical without Feedback	1.19	0.12
Hierarchical with Feedback	1.03	0.04

VII. Conclusions

This paper studied the PoA in active signal landscape map building of environments comprising multiple receivers with *a priori* knowledge about their own states and multiple unknown terrestrial stationary SOPs. The objective of such maps are to enable non-GNSS SOP-based navigation and remove the dependency on GNSS signals. Four information fusion and decision making architectures were studied: decentralized, centralized, and hierarchical (with and without feedback). It was demonstrated that the hierarchical with feedback architecture performed comparably to the centralized architecture.

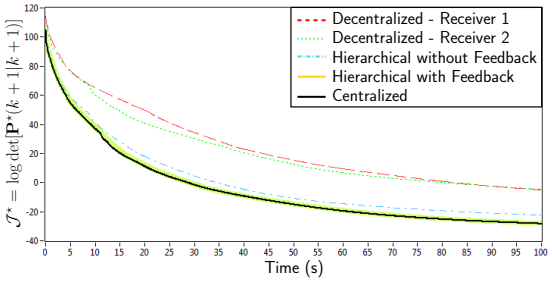

Fig. 4. Signal landscape map uncertainty

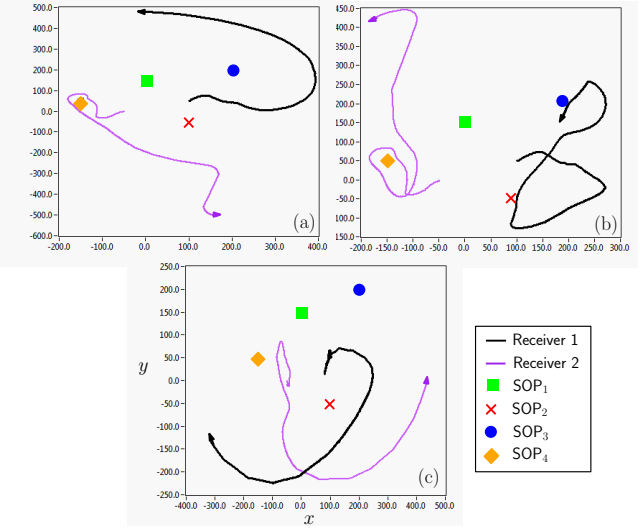

Fig. 5. Receiver trajectories for (a) centralized, (b) hierarchical with feedback, and (c) decentralized and hierarchical without feedback architectures

References

[1] K. Pesyna, Z. Kassas, J. Bhatti, and T. Humphreys, "Tightly-coupled opportunistic navigation for deep urban and indoor positioning," in *Proc. of ION GNSS*, Sep. 2011, pp. 3605–3617.

[2] Z. Kassas, "Collaborative opportunistic navigation," *IEEE Aerospace and Electronic Systems Magazine*, vol. 28, no. 6, pp. 38–41, Jun. 2013.

[3] Z. Kassas and T. Humphreys, "Observability analysis of opportunistic navigation with pseudorange measurements," in *Proc. of AIAA Guidance, Navigation, and Control Conference*, Aug. 2012, pp. 4760–4775.

[4] ——, "Observability and estimability of collaborative opportunistic navigation with pseudorange measurements," in *Proc. of ION GNSS*, Sep. 2012, pp. 621–630.

[5] ——, "Observability analysis of collaborative opportunistic navigation with pseudorange measurements," *IEEE Trans. on Intelligent Transportation Systems*, 2013, in press.

[6] ——, "Motion planning for optimal information gathering in opportunistic navigation systems," in *Proc. of AIAA Guidance, Navigation, and Control Conference*, Aug. 2013, pp. 4551–4565.

[7] ——, "Receding horizon trajectory optimization for simultaneous signal landscape mapping and receiver localization," in *Proc. of ION GNSS*, Sep. 2013.

[8] ——, "Greedy motion planning for simultaneous signal landscape mapping and receiver localization," *IEEE Trans. on Aerospace and Electronic Systems*, 2013.

[9] E. Koutsoupias and C. Papadimitriou, "Worst-case equilibria," in *Porc. of 16th Annual Symposium on Theoretical Aspects of Computer Science (STACS)*, Mar. 1999, vol. 1563, pp. 404–413.

[10] Y. Bar-Shalom, X. Li, and T. Kirubarajan, *Estimation with Applications to Tracking and Navigation*. New York, NY: John Wiley, 2002.

[11] S. Julier and J. Uhlmann, "A non-divergent estimation algorithm in the presence of unknown correlations," in *Proc. of American Control Conference*, vol. 4, Jun. 1997, pp. 2369–2373.

[12] H. Durrant-Whyte, *Multi Sensor Data Fusion*, 2001.

[13] G. Mutambara, *Decentralized Estimation and Control for Multisensor Systems*. CRC Press, 1998.